Physics of organic-organic interfaces

Jarzab, Dorota Maria

Chapter 1
Introduction

This chapter offers a brief introduction to organic semiconductors, to the phenomena that occur at organic-organic interfaces, and to the methods that allow investigation of the processes determining the performance of organic devices. Following a discussion of the main aspects, an overview of the thesis is given.

1.1 Plastic electronics for future technology

In 1891, Bolesław Prus* spun tales about the coming age. "What an age…without leaving Warsaw, we will be able to explore in a few minutes Lapland and the Sahara, enjoy the opera in Paris or the explosions of the volcano Krakatoa." Prus's visions must have seemed mere literary fantasy to many of his contemporaries. Today, the possibility of experiencing the farthest corners of the World in real time via television or the Internet is so accessible that we do not even consider it special. It is an integral part of our daily lives.

Often in history what once was considered impossible or fantastic eventually becomes possible and ordinary, generally thanks to the work of scientists.

Let us now imagine our monthly expenses without an electricity bill. Hard to believe, perhaps, but this is actually possible today, because the windows in our homes can generate electricity, setting us free from the power grid. Imagine enjoying a holiday camping in a wilderness area surrounded by breathtaking mountains. Even if no power supply is available, we still will be able to use our mobile phones or our cameras regardless the charge in the batteries. It is possible because we have incorporated portable solar battery chargers into our backpacks. Imagine as well that after hiking all day, we sit in front of our campfire while reading a book. We've downloaded our favourite writer's last novel on our A4-size electronic paper, which is both very light and can be easily rolled-up, so there was no a concern about available space in our backpack. And once we've finished reading the novel we might download a different book, or chat with friends still at work, or follow the latest news.

The scenes described above might appear to belong to fiction. In reality, the prototypes of these products are already available. The realization of these and many other innovative devices is possible thanks to organic semiconductors, which can be considered simply as semiconducting plastics. Organic semiconductors, compared to traditional inorganic semiconductors like silicon or gallium arsenide, are flexible and lightweight and can be semitransparent. Additionally, they can be printed on large plastic sheets by using techniques similar to those used to print magazines and newspapers, resulting in a relatively low-cost manufacturing process. These printing methods enable electronics to be used for a wide range of applications unthinkable with traditional processing methods.

However, before these and many other products become a daily reality much effort is required. Not all organic semiconductors-based devices perform

* Boleslaw Prus pen name of Aleksander Glowacki (1847-1912); Polish writer, essayist, and novelist of the period of positivism; co-founder of Polish realism, chronicler of Warsaw, thinker and promoter of knowledge, and social activist.

sufficiently to be of commercial interest. Although plastic semiconductors have been extensively studied since the 1970s, when Shirakawa, MacDiarmid and Heeger demonstrated that the conductivity of conjugated polymers can be controlled by doping,[1] several aspects must still be improved. The understanding and the control of the processes determining the properties of organic semiconductors is crucial to the further development of plastic electronics and to enable their widespread commercialization.

In this PhD thesis I present the experimental study of a variety of organic-organic heterojunctions that have applications in organic devices. By combining spectroscopy and microscopy techniques, I investigated the nature of the interactions between the materials and the influence on the final properties of the heterojunction.

1.2 Organic semiconductors

The general term organic semiconductors define a large family of organic materials that exhibit semiconducting properties. We can distinguish two main classes of organic semiconductors: low molecular weight materials (oligomers) and polymers. The common characteristic of both classes is the arrangement of the carbon atoms in a series of alternating single and double bonds (Figure 1.1(a)), also called conjugation.

In a conjugated system, carbon atoms are sp^2-hybridized (the 2*s* orbital is mixed with only two of the three available 2*p* orbitals) which means that only three σ bonds can be formed, leaving the p_z orbital unaltered. The mutual overlap between unhybridized p_z orbitals of adjacent carbons leads to the formation of π bonds. The electrons of overlapping p_z orbitals form a delocalized electronic orbital over the whole conjugation length (Figure 1.1 (b)). These delocalized π orbitals are at the origin of the semiconducting properties of this class of materials.

While both the σ and the π bonds have covalent nature, when organic molecules meet to form solids they are kept together by weak van-der-Waals bonds. The consequences of this considerably weak intermolecular interaction in organic materials are reflected not only in the mechanical and thermodynamic properties of organic semiconductors, but as well in the weaker electronic delocalization of wave function. This has direct implications for charge transport and optical properties.

The lowest electronic excitation of conjugated molecules is the π-π* transition. This transition leads to the formation of an electron-hole pair kept together by Coulomb force. The energy difference between the π band, which is the highest

occupied molecular orbital (HOMO), and the π* band, which is the lowest unoccupied molecular orbital (LUMO), is generally in the range between 1.5 – 3 eV;[2] thus the π-π* transition is possible, for example, upon light absorption.

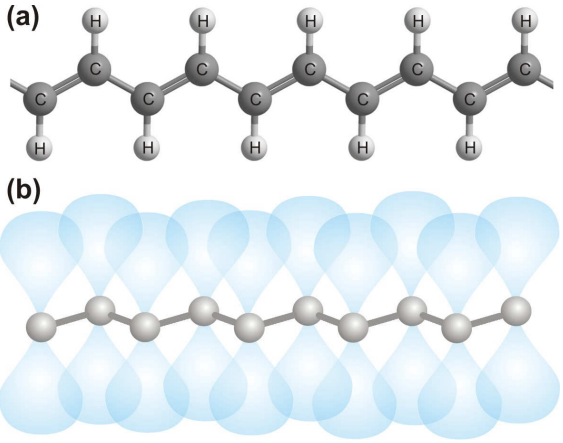

Figure 1.1. (a) Single and double bounds alternation in polyacetylene; (b) Schematic representation of the π delocalized electronic orbitals.

The unique properties of this class of materials make them attractive alternatives to epitaxially grown purely inorganic layers, especially for application in such optoelectronic devices as: solar cells,[3],[4],[5] light emitting diodes (LEDs),[6],[7],[8] and transistors (FETs).[9],[10]

1.3 Organic-organic heterojunctions

Inorganic semiconductor electronic and optoelectronic devices are generally composed of p-n heterostructures. Although the physics governing organic and inorganic semiconductors is very different, also in the case of organic semiconductors, heterojunctions formed by dissimilar materials are used as active layers in electronic devices.

We can distinguish two main types of organic heterojunctions: (i) planar heterojunctions, formed by multilayer structures (Figure 1.2 (a)), and (ii) three dimensional diffused heterostructures, often called bulk heterojunctions (Figure 1.2 (b)).

Planar heterojunctions are fabricated by vacuum depositing successive small molecule layers, or by processing from solution successive polymer or small molecule layers. These multilayer systems are mainly used in LEDs to improve the

electroluminescence efficiency optimizing every layer for a certain role, e.g: electron and hole transport, emission, blocking of opposite charges, etc.[11-13]

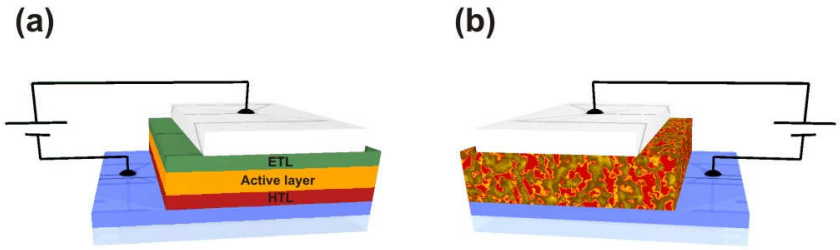

Figure 1.2. Example of devices with planar (a) and bulk heterojunction (b) as active layer; ETL – electron transport layer; HTL – hole transport layer; Active Layer-electroluminescent layer

The second type of heterostrucure-bulk heterojunction-is obtained by blending two or more materials in common solvents. This strategy takes advantage of the most unique property of organic semiconductors-their solubility-and allows for the production of new solid composites with specific physical properties without the synthesis of new material. For instance, organic materials usually show unipolar charge transport, with holes or electrons as dominant charge carriers. Mixing of p-type and n-type semiconductors together enables active layers showing ambipolar transport characteristics. This feature is particularly desired in the fabrication of FETs[14] for application in flat panel displays[15] or integrated circuits.[16]

For applications in light emitting diodes, blending different materials not only achieves good and balanced hole and electron transport, but also allows for the possibility of fabricating devices showing any color of emission, including white.[17][18] This is made possible by mixing materials having different band gaps, and consequently showing emission in different parts of the visible spectrum.
Moreover, bulk heterojunctions have a significant advantage over the single layer in photovoltaics. In solar cells, the use of organic semiconductor materials with electron acceptor and electron donating properties and good electron and hole mobility is necessary for efficient charge separation and conduction.[19]

1.4 Physical phenomena at organic-organic interfaces

Organic-organic interfaces are inherent for plastic electronics. The quality and quantity of the interfaces, especially in bulk heterojunctions, determines to a large extent a device's performance and efficiency. Because of the intermolecular interactions in these interfaces, novel phenomena and various types of excited

states emerge. In the following, a short description of processes and phenomena studied in this thesis is presented.

1.4.1 Förster Energy Transfer

Förster Energy Transfer[20] is a nonradiative process based on a long-range dipole-dipole interaction. In this process the electronic excitation is transferred from the donor molecule to the acceptor molecule (Figure 1.3(a)). Förster Energy Transfer can occur in a donor-acceptor system when: (i) the emission spectrum of the acceptor overlaps with absorption spectrum of the donor; (ii) the distance between the donor and acceptor is smaller than about 10Å.[21] This process can be exploited in the fabrication efficient LEDs, in particular white LEDs.

1.4.2 Charge Transfer

The process of the transfer of an electron or hole from the excited molecule to its neighbouring molecule is called charge transfer (Figure 1.3(b)). It occurs at the interface between molecules (donor and acceptor) having different ionization potentials and electron affinities. The energy difference between HOMO levels (for hole transfer) or between LUMO levels (for electron transfer) at the interface should be bigger than the exciton binding energy, which in organic materials is ~ 0.3 – 0.5 eV.[22] In optimized systems charge transfer at the donor-acceptor interface happens on a femtosecond time scale.[23] Efficient charge transfer is required in photovoltaic devices in order to split the photogenerated exciton into free charges.

1.4.3 Charge transfer excitons

Charge transfer (CT) excitons are weakly bound electron-hole pairs located at the interfaces of adjacent different molecules. CT excitons are ground state interactions formed at the interface between molecules with dissimilar electron affinity. The excited version of this interaction is called exciplex and is formed when the electron is transferred from the excited molecule to its neighbouring molecule, but remains coloumbically correlated with the hole in the parent hole.
Both states have lower energy than the optical band gap, and this can be seen in the photoluminescence spectra as a new emission peak, red shifted with respect to the singlet emission.

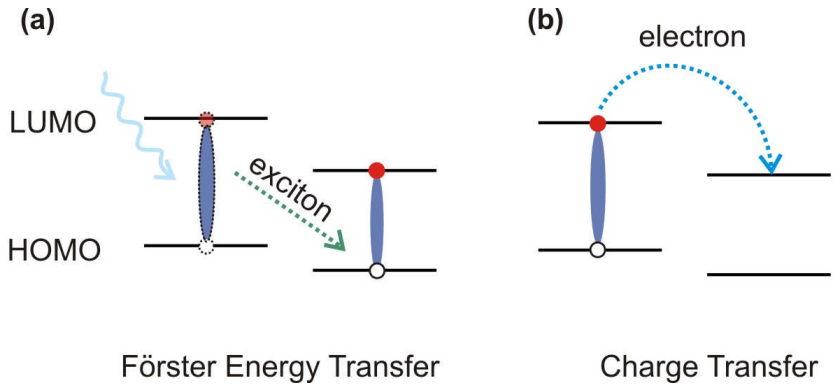

Figure 1.3. Schematic illustration of Förster Energy Transfer (a) and charge transfer (b) in donor-acceptor systems.

1.4.4 Excimers

Excimers are formed by interaction of two molecules of the same kind, one molecule in the electronically excited state and the other in its ground state. Excimers exist only in the excited state. Their luminescence spectrum is characterized by a broad red-shifted emission with a long decay time with respect to the isolated molecule.

1.5 Photophysics and morphology of bulk heterojunctions

Insight into the working mechanism and a phenomenon occurring at the organic interfaces is crucial for the further development of plastic electronics. Because organic semiconductors show strict correlation between electronic and optical properties, and supra-molecular arrangements and a device's performance, there is a need to study and correlate all these aspects by means of a multidisciplinary study, combining spectroscopic and morphological analysis techniques.

1.5.1 Steady state and time resolved photoluminescence

Photoluminescence measurements are one of the most informative techniques for investigating phenomena and electronic excited states in organic semiconductors.[24] In particular, time resolved photoluminescence is a very powerful tool, in that it allows an understanding of the dynamics of the processes occurring in the materials. In this technique a sample is excited with a short pulse of monochromatic light and then the subsequent photoluminescence decay is

measured as a function of time. By analyzing the decay time of the excitation we can gain knowledge about the nature of the excited states and understand the various routes of energy losses in the material.

The fundamental excitations in organic semiconductor films are Frenkel excitons.[25] Typically, the electron and hole forming the exciton are located on the same molecule, and Frenkel excitons are therefore characterized by a small radius (<5 Å) with strong binding energy (0.3 – 0.5 eV). Depending on the relative orientation of the electron and hole spin, the exciton may be singlet (total spin S = 0) or triplet (total spin S = 1).

In general, when we consider a single molecule, it is more correct to speak about excitation than about excitons, because the exciton is simply a collective excitation. An organic molecule can be considered as three-level system (Figure 1.4) with the electronic ground state (S_o) and two first excited state singlet (S_1) or triplet (T_1).

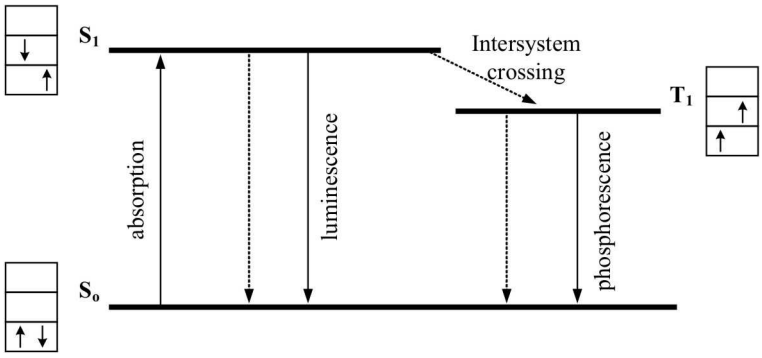

Figure 1.4. Simplified schematic representation of the energy levels and depopulation routes for a single molecule.

In time resolved PL experiments excitation usually promotes the molecule from its ground singlet state (S_o) to the first excited singlet state (S_1). The depopulation of this state can occur: i) by rapid recombination to the S_o state via radiative (luminescence) or nonradiative transitions; ii) by intersystem crossing to the triplet state (T_1), followed by radiative (phosphorescence) or nonradiative recombination to the S_o state. For organic molecules generally, the probability of the intersystem crossing is rather low, the lifetime of triplet typically is very long (10^{-3} – 10 s), and radiative decay is usually not observed at room temperature.

In molecular aggregates, where the collective response to excitation is called an exciton, the properties of the PL emission depend not only on the electronic structure of the single molecule, but are also strongly influenced by the molecular packing and coupling in the solid. Thus, by analyzing the PL emission we can obtain information about molecular orientation in thin films. For instance, when

two identical molecules are close to each other in a spatial arrangement, the excitation energy level splits due to the interactions between them and causes a spectral shift with respect to the single molecule.

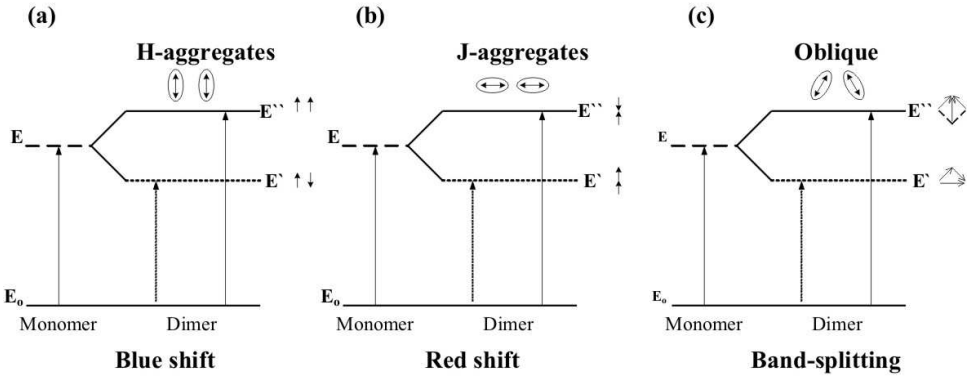

Figure 1.5. Electronic level splitting in dimers for different dipole geometries: (a) parallel; (b) antiparallel; (c) oblique. Dimer refers to two identical molecules (two monomers) being in close spatial arrangement. (Taken from M. Pope[25])

When the transition dipoles of both molecules are parallel (H-aggregates, Figure 1.5(a)) or they have head-to-tail arrangement (J-aggregates Figure 1.5(b)) only one excited state has nonzero transition moment and is optically dipole-allowed, resulting in an energy increase (blue-shift) or decrease (red-shift), respectively. In the case of oblique dipoles (Figure 1.5(c)) both excited states have nonzero transition moment and are optically dipole-allowed. In this instance band splitting occurs and both states can radiate.

In semiconducting organic thin films the emission from the S_1 level is characterized by a photoluminescence decay time in the order of nano- or picoseconds. For organic heterojunctions we can usually detect a reduction of the decay time caused by interaction with molecules having different electron affinity and ionization potential. For example, in donor-acceptor systems we can observe significant reduction of the PL decay time with respect to the decay time of the pristine donor due to charge transfer. The reduction of the PL decay time can also be caused by Förster Energy Transfer; however, in this case, apart from the quenching of the donor emission, we also expect a delayed (rise time) acceptor emission.[26]

1.5.2 Morphology

The morphology of organic thin film is one of the most important parameters determining the device's efficiency.[27],[28] There is therefore a need to study

molecular orientation, phase segregation or local chemical composition and to correlate it with photophysical properties and a device's performance. Unfortunately, there is no experimental technique that can provide complete information about thin film structure and composition. In this PhD study several different techniques were used to determine these thin film properties.

Surface topography information was obtained with atomic force microscopy (AFM) operating in tapping mode. This technique provided high-resolution surface topography images, complete with phase images, which reflects the material surface properties, such as stiffness, viscoelasticity or chemical composition.[29]

Information about the depth profile of the thin film was obtained by high-kinetic-energy X-ray photoelectron spectroscopy (XPS). Photoelectron spectroscopy is a technique that based on the Einstein's photoelectric effect, i.e. the electron can escape from the system if absorbs energy higher than the ionization potential. In this technique, sample is irradiated by monochromatic light, which causing the ejection of core-level electrons. Next, the kinetic energy distribution of outcoming electrons is measured. Because each element has its characteristic binding energy, by analysis of photoelectron spectra we can obtain information about chemical composition of the surface. Additionally, the peak shape and precise position give information about the chemical state of the elements. The probing depth is different for different materials and depends on the energy of the exciting photons.

A scanning near-field optical microscope (SNOM) was used to correlate film morphology with photoluminescence properties. SNOM is a scanning-probe technique which allows measure the optical properties of the sample in the scale much smaller than diffraction limit. This is possible by exploiting the properties of the evanescent wave. Because the evanescent wave decays exponentially with a distance less than the wavelength of the light, to utilize its attributes is necessary to place a sample within the near-field distance of the source light. The resolution of SNOM is defined by the size of the light source, thus to measure below diffraction limit is necessary to use as light source (probe) with sub-wavelength diameter aperture. There is several ways to realize a sub-wavelength diameter probe. We used a method based on a standard AFM cantilever with a hole in the centre of the pyramidal tip, with a laser light focuses on this hole. The incorporation of the SNOM into the AFM allows obtain optical information correlated with topography image.

1.6 Experimental

In this thesis several different experimental techniques were used to study the properties of organic materials. In the following, a short description of the most frequently used experimental set-ups is given.

1.6.1 Photoluminescence measurements

A schematic drawing of the experimental set-up for PL measurements is shown in Figure 1.6. For steady state and time resolved PL measurements samples were excited by the second harmonic of a mode-locked Ti:sapphire laser tunable in the range ~720-980 nm, delivering pulses of 150 fs, with repetition frequency of ~76 MHz. To vary the repetition rate of the exciting pulse, an optical pulse selector with the division ration between 1:20 to 1:5000 was used.

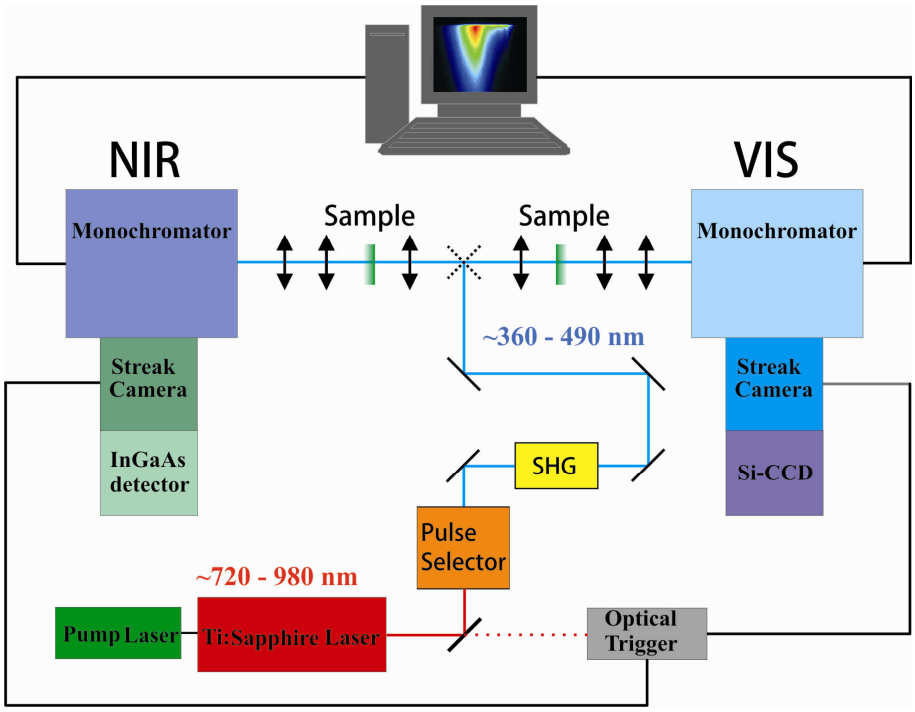

Figure 1.6. Scheme of the photoluminescence time resolved experimental set-up. Depending on the emission properties of a sample, photoluminescence signal is measured by the detecting system working in the visible spectral range (right site) or by the detecting system working in the near-infrared (left site). Arrows represents lenses.

Ti:sapphire laser was pump with solid-state diode-pump, frequency-doubled Nd:Vanadate (Nd:YVO_4) laser, providing single-frequency green (532 nm) output at power 5 Watts.

The time resolved PL signal was recorded with two Hamamatsu streak cameras, one with a photocathode sensitive in the visible, and the other in the near-infrared spectral range. The operation principle of this instrument is shown on Figure 1.7. The measured light (represented here by four pulses with different optical intensity, spectral position and arrival time) first passes through an entrance slit, next by the optics the slit image is formed on the photocathode. The photocathode converts the incident light into a number of electrons proportional to the light intensity. The converted electrons pass between two sweep electrodes, where they are deflected from the horizontal direction at different angles, depending on their arrival time. Next, the deflected electrons pass the micro-channel plate (MCP), where they are multiplied several thousand times, and at the end electrons are converted again into light on the phosphor screen. The vertical direction on the phosphor image serves as the time scale, and the horizontal as the space scale. Depending on the PL lifetime, the streak cameras were used in single-sweep or in synchroscan mode. In single-sweep mode a ramp voltage is applied to the sweep electrodes and only single sweep is involved. In this mode, the measurement range is from 5 ns to 10 ms. In synchroscan mode, high-speed repeated sweep is used, in which a highfrequency sinewave voltage is applied to the deflection electrodes (Figure 1.7)). In this mode we measured signal in the range between ~160 ps and ~2200 ps. The timing of the streak sweep is controlled by the trigger; voltage applied to the sweep electrodes is synchronized to the incident light.

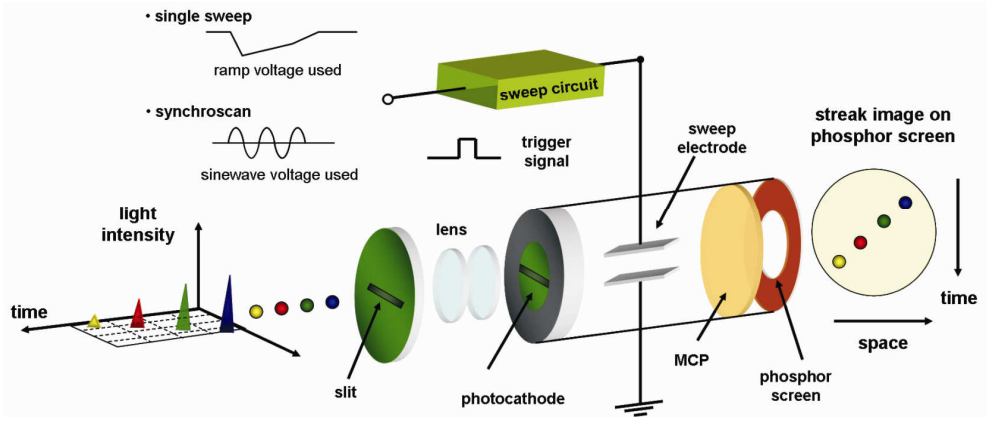

Figure 1.7. Operation principle of the Streak Tube.

The steady state PL spectra were detected in the visible with Si-CCD from Hamamatsu and in the near-infrared with InGaAs detector from Andor. The PL spectra were corrected for the spectral response of the set up, which was determined with quartz tungsten halogen calibration lamp.
All PL decays were fitted with the function:

$$I_{PL}(t) = \sum_i A_i \cdot \exp\left(-\frac{t}{\tau_i}\right)$$

where, A_i, and τ_i are fitting parameters; i=1 for monoexponential decay, and i=2 for biexponential decay.
The rise time was fitted with the function:

$$I_{PL}(t) = \left[A_1 + A_2 \cdot \left(1 - \exp\left(-\frac{t}{\tau_{Rise}}\right)\right)\right] \cdot \exp\left(-\frac{t}{\tau_{Decay}}\right)$$

where, A_1, A_2 and τ_1, τ_2, τ_{Rise}, τ_{Decay}, are fitting parameters.
Absorption spectra were recorded with Perkin-Elmer Lambda 900 Spectrometer.

1.6.2 Microscopies

For near-field measurements a Witec SNOM was used. This instrument allows measuring simultaneously the local photoluminescence and the topography of the sample surface with a spatial resolution of ~100 nm. The scheme of experimental set-up is shown in Figure 1.8. The probe (tip) had a hollow pyramid mounted on a silicon cantilever, similar to the one used in AFM. The pyramid coated with aluminum had a hole at the apex with a diameter of <100 nm. To control tip-sample distance the feedback system similar like in AFM was used. Samples were excited with the 454 nm line of argon-ion laser. The excitation laser was aligned with the hole of the cantilever, and the beam of the feedback laser was shifted of about 50 μm from the excitation laser. SNOM measurements were performed in transmission mode, and images were recorded by collecting the PL spectra point by point with a monochromator coupled with a CCD camera.
Atomic force microscopyimages were taken on a MultiMode AFM with a NanoScope IV Scanning Probe Microscope Controller, mounting Si cantilevers, and operated in tapping mode.
All SNOM and AFM data were taken in ambient conditions.

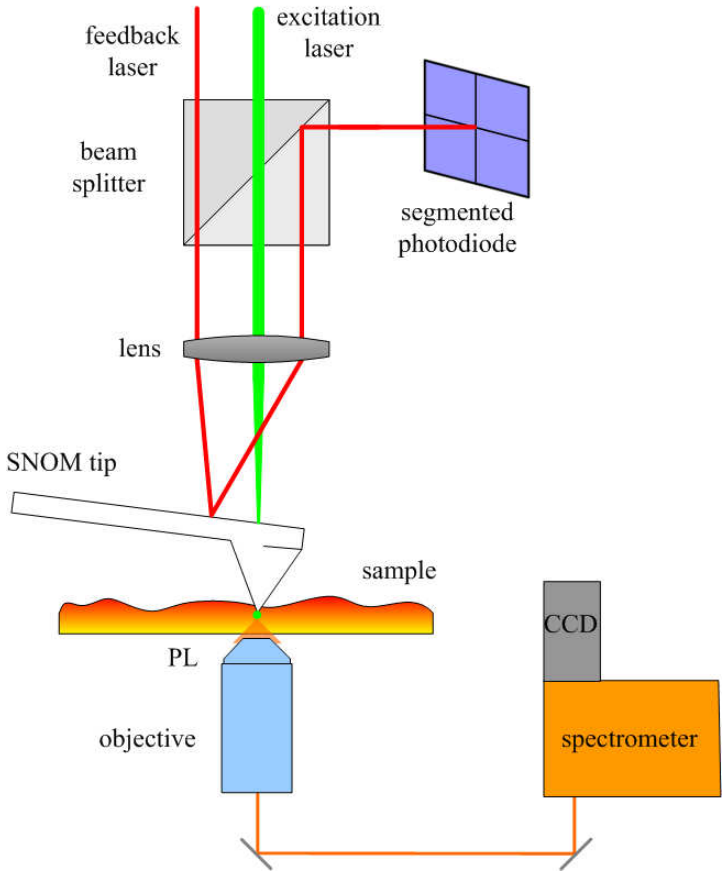

Figure 1.8. Schematic of the working mechanism of SNOM.

1.7 Samples fabrication

All samples studied in this work were processed from solution, by using different fabrication methods.

1.7.1 Spin coating

In this procedure, an excess amount of a solution is cast on the substrate, next the substrate is accelerated to its final rotational speed. During the spinning time solvent evaporates, and the thin film is formed. The quality of the thin film in big extend is affected by the spinning parameters, i.e. acceleration, spinning speed and time of the spinning, and also by the concentration of the solution and the vapour pressure of the solvent.

1.7.2 Doctor blade coating

In this technique, the solution is placed in a narrow slit between the surface of the substrate and a blade. Next, the blade is dragged at a constant velocity over the substrate and a thin film is formed. The parameter that determine the film properties (besides the concentration of the solution and the vapour pressure of the solvent) are: the size of the slit between blade and substrate, the speed of the blade and the temperature of the bed, where the substrate is placed.

In some cases, after processing from solution thin films were thermally annealed, i.e. a heat treated in a glove-box filled with nitrogen or in a vacuum oven. For samples studied in this thesis, the annealing temperature was in the range of 110-140ºC.

1.7.3 Slow drying

In this protocol, the samples, after drop-casting deposition or spin coating with low speed (spin speed < 1000 r.p.m.) obtained from a solution using a low vapour pressure solvent, are left to dry in a closed Petri dish. The drying process that occurs in solvent-vapour-saturated atmosphere is called solvent annealing.

1.8 Outline of the thesis

This thesis focuses on studying the nature of the phenomena that occur at organic-organic interfaces and on their effect on the ultimate properties of the heterojunction. We present a comprehensive study of a variety of organic heterojunctions, having applications in light emitting diodes (Chapter 2), field effect transistors (Chapter 3) and solar cells (Chapter 4, 5 and 6). Moreover, in Chapter 7, we investigate an inorganic-organic hybrid heterojunction that has application in near-infrared photodiodes.

Chapter 2, is devoted to the investigation of a polymer-polymer blend that has application in the fabrication of white light emitting diodes. In recent years, the application of LEDs for displays or lighting has held a lot of interest, due to the potential energy saving they offer. To achieve highly efficient organic light emitting diodes, very often it is necessary to blend materials having complementary properties. For example, achieving white LEDs requires excitonic recombination in different part of the visible spectrum, which can be realize by blending together different emitters, each one having different band gap. Optoelectronic devices using organic blends as active layer show a high correlation between the heterostructure morphology and the devices performance, thus, it is very important

to study both the heterostructure conformation and the electronic interaction of the components. In Chapter 2, we present a combined photoluminescence and morphological study of a host-guest polymer blend that finds application in light emitting diodes. This investigation allowed us to gain insight into the emission properties and mechanism of this polymer-polymer blend. Steady-state and time-resolved photoluminescence measurements evidence partial Förster energy transfer. Atomic force microscopy on blends with different weight ratios of host and guest polymers showed the presence of two phases. The nature of the phases was identified by means of scanning near-field optical microscopy.

Next chapter is devoted to the study of molecular thin films used to fabricate high performing n-type organic field effect transistors (OFETs). OFETs are inherent part of complementary metal oxide semiconductor circuits (O-CMOS), which are the basic elements of many electronic devices. In Chapter 3, we reported the realization of bottom-contact bottom-gate OFETs based on spin-coated films of perylene derivatives, which combines solution-processability characteristics and excellent semiconductor properties with electron mobilities up to 0.15 $cm^2V^{-1}s^{-1}$. In this chapter, we describe studies of the influence of different supramolecular arrangements in the organic layer of small molecules on the transistor performance. The devices based on spin-coated films of fluorocarbon functionalized perylene were found to have better performances after thermal treatment. We attributed this improvement to the high crystallinity and to the edge-on orientation promoted by the annealing, as shown by confocal laser microscopy. Next, we compared the transistor performance of two solution-processed perylene derivatives. The fluorocarbon functionalization of the aromatic core versus the hydrocarbon-functionalization improves the electron mobility by one order of magnitude. This increase is ascribed to a higher degree of supramolecular order in the thin films, which is evidenced by time resolved photoluminescence.

Organic semiconductors attract a lot of attention in application for photovoltaic devices. This is caused mainly by the increasing energy demand and the need for renewable energy production. Silicon-based solar cells are very expensive due to their high production cost. Thus organic-based photovoltaics, which can be fabricated by low-cost manufacturing methods, are seen as promising candidates for energy production. So far, the best performing organic solar cells use polymer-fullerene (donor-acceptor) bulk heterojunction as the active layer. In short, the working mechanism of this kind of devices can be described in 4 steps: (i) exciton generation in donor material; (ii) exciton diffusion toward a quenching site (iii) charge separation and electron transfer to an acceptor and (iv) charge transport toward respective electrodes. The two main requirements for highly performing organic solar cells are efficient charge separation and transfer. In this thesis, we

focused on the study of charge separation process and the relation of the charge separation and the morphology of the thin film.

In Chapter 4, we investigate the influence of the reduction of the LUMO offset on the efficiency of charge transfer in bulk heterojunctions. The energy alignment between donor and acceptor is one of the parameters determining the performance of this kind of devices. We studied two bulk heterojunctions with LUMO offset of ~1.1 eV and ~1.0 eV. The photoluminescence properties were measured in thin films prepared by different protocols, thus having different microstructure of the bulk heterojunction, and in solutions, where the donor-acceptor distribution is homogeneous. Thin films of bulk heterojunction with LUMO offset of 1.0 eV showed slower photoluminescence dynamics than the one with the offset of 1.1 eV. In solution, the two blends exhibited the same photoluminescence decay time, indicating that the variation of the energy level offset of ~100 meV does not play a detrimental role in the efficiency of the charge transfer. The slower dynamics in the bulk heterojunction with LUMO offset of 1.0 eV was ascribed to radiative losses caused by the non-optimal three-dimensional architecture in the film.

Generally, the structure of the bulk-heterojuction is investigated in in-plane morphology; however, the knowledge about the depth profile of the thin film is also important, in particular, the vertical phase segregation can determine a non-optimal interface with the anode or cathode. In Chapter 5, the vertical phase separation of a bulk heterojunction used for organic solar cells was investigated by high-kinetic-energy X-ray photoelectron spectroscopy at different photon energies. With this technique we show that the topmost layer of bulk heterojunction is formed only by the polymer (donor), and that the acceptor (fullerene) is present only at a depth which goes beyond a few nanometers.

In Chapter 6, photoluminescence studies of charge transfer exciton emission in bulk heterojunctions using as donor a narrow-band-gap semiconductor is presented. Charge transfer excitons (CTE) are interfacial states that have a lower binding energy respect to Frenkel excitons. The understanding of the nature and role of those interfacial states holds crucial relevance for the further development of solar cells. Photoluminescence measurements on thin films with increasing acceptor percentage show a red-shift of the charge transfer emission in agreement with the increase of the average dielectric constant of the medium. Low temperature measurements revealed that while the dynamics of the singlet exciton is longer at low temperature, the dynamics of the charge transfer emission is temperature independent. This behaviour rules out any diffusion process of the CTE and energy transfer from this state towards other states. Moreover, the photoluminescence measurements performed under bias showed that the charge transfer population is bias dependent; however, at the bias of functioning of the solar cells still the charge transfer exciton recombination represent a loss for the device.

In the last chapter, we presented the investigation of the working mechanism of the hybrid ternary blend that has shown excellent performance when used as active layer in NIR photodiodes. This class of hybrid devices have active layer composed of a mixture of solution-processed inorganic nanocrystals (NCs) and an organic semiconductors. The possibility to process from solution both NCs and organic semiconductors provides opportunity to obtain a new and versatile class of hybrid materials. The final prospective is to be able to merge the advantages of both materials classes, e.g., the high stability of inorganic crystals with the full tunability and mechanical properties of the organic materials. A further development of hybrid devices demands the study and the understanding of the processes occurring in hybrid heterojunction. In particular it is crucial to investigate the aspects that in large extend determine the devices performance, such as charge separation and charge transfer processes. In Chapter 7, we described how we investigated the working mechanism of the hybrid ternary blend composed of inorganic nanocrystals and polymer-fullerene bulk heterojunction. Photoluminescence dynamics were used to understand the role of each component, both in the visible and near-infrared spectra range. In the ternary blend the efficiency of the charge transfer is significantly enhanced compared to the two binary blends PbS:P3HT and PbS:PCBM, indicating that both hole and electron transfer from excited NCs to the polymer and fullerene occur, respectively

References

[1] C. K. Chiang, C. R. Fincher, Y. W. Park, A. J. Heeger, H. Shirakawa, E. J.Louis, S. C. Gau, A. G. MacDiarmid, *Phys. Rev. Lett.* **1977**, *39*, 1098.

[2] W. Brütting, *Physics of Organic Semiconductors*, Wiley-vch, **2005**.

[3] P. Peumans, A. Yakimov, S. R. Forrest, *J. Appl. Phys.* **2003**, *93*, 3693.

[4] A. Hadipour, B. de□Boer, P. Blom, *Adv. Funct. Mater.* **2008**, *18*, 169-181.

[5] L. Chen, Z. Hong, G. Li, Y. Yang, *Adv. Mater.* **2009**, *21*, 1434-1449.

[6] J. H. Burroughes, D. D. C. Bradley, A. R. Brown, R. N. Marks, K. Mackay, R. H. Friend, P. L. Burns, A. B. Holmes, *Nature* **1990**, *347*, 539-541.

[7] S. Reineke, F. Lindner, G. Schwartz, N. Seidler, K. Walzer, B. Lussem, K. Leo, *Nature* **2009**, *459*, 234-238.

[8] J. Wu, M. Agrawal, H. A. Becerril, Z. Bao, Z. Liu, Y. Chen, P. Peumans, *ACS Nano* **2010**, *4*, 43-48.

[9] F. Garnier, R. Hajlaoui, A. Yassar, P. Srivastava, *Science* **1994**, *265*, 1684-1686.

[10] D. Braga, G. Horowitz, *Adv. Mater.* **2009**, *21*, 1473-1486.

[11] A. Brown, N. Greenham, J. Burroughes, D. Bradley, R. Friend, P. Burn, A. Kraft, A. Holmes, *Chem. Phys. Lett.* **1992**, *200*, 46-54.

[12] M. Muccini, R. F. Mahrt, R. Hennig, U. Lemmer, H. Bässler, F. Biscarini, R. Zamboni, C. Taliani, *Chem. Phys. Lett.* **1995**, *242*, 207-211.

[13] S. Sax, N. Rugen-Penkalla, A. Neuhold, S. Schuh, E. Zojer, E. J. W. List, K. Müllen, *Adv. Mater.* **2010**, *22*, 2087-2091.

[14] J. Wang, H. Wang, X. Yan, H. Huang, D. Yan, *Appl. Phys. Lett.* **2005**, *87*, 093507.

[15] H. Huitema, G. Gelinck, J. van der Putten, K. Kuijk, C. Hart, E. Cantatore, D. de Leeuw, *Adv. Mater.* **2002**, *14*, 1201-1204.

[16] B. Crone, A. Dodabalapur, Y. Lin, R. W. Filas, Z. Bao, A. LaDuca, R. Sarpeshkar, H. E. Katz, W. Li, *Nature* **2000**, *403*, 521-523.

[17] C. D. Muller, A. Falcou, N. Reckefuss, M. Rojahn, V. Wiederhirn, P. Rudati, H. Frohne, O. Nuyken, H. Becker, K. Meerholz, *Nature* **2003**, *421*, 829-833.

[18] J. Huang, G. Li, E. Wu, Q. Xu, Y. Yang, *Adv. Mater.* **2006**, *18*, 114-117.

[19] C. J. Brabec, S. E. Shaheen, T. Fromherz, F. Padinger, J. C. Hummelen, A. Dhanabalan, R. A. J. Janssen, N. S. Sariciftci, *Synth. Met.* **2001**, *121*, 1517-1520.

[20] T. Forster, *Discuss. Faraday Soc.* **1959**, *27*, 7-17.

[21] E. Moons, *J. Phys.: Condens. Matter* **2002**, *14*, 12235-12260.

[22] J. J. M. Halls, J. Cornil, D. A. dos Santos, R. Silbey, D. Hwang, A. B. Holmes, J. L. Bredas, R. H. Friend, *Phys. Rev. B* **1999**, *60*, 5721.

[23] N. S. Sariciftci, L. Smilowitz, A. J. Heeger, F. Wudl, *Science* **1992**, *258*, 1474–1476.

[24] N. Sariciftci, L. Smilowitz, A. Heeger, F. Wudl, *Synth. Met.* **1993**, *59*, 333-352.
[25] M. Pope, C. E. Swenberg, *Electronic Processes in Organic Crystals and Polymers*, Oxford University Press, **1999**.
[26] C. Botta, G. Patrinoiu, P. Picouet, S. Yunus, J. -E. Communal, F. Cordella, F. Quochi, A. Mura, G. Bongiovanni, M. Pasini, et al., *Adv. Mater.* **2004**, *16*, 1716-1721.
[27] H. Hoppe, N. S. Sariciftci, *J. Mater. Chem.* **2006**, *16*, 45.
[28] Y. Shi, J. Liu, Y. Yang, *J. Appl. Phys.* **2000**, *87*, 4254.
[29] D. Raghavan, X. Gu, T. Nguyen, M. VanLandingham, A. Karim, *Macromolecules* **2000**, *33*, 2573-2583.